

Symmetry protected skyrmions in 3D spin-orbit coupled Bose gases

Guanjun Chen,^{1,2} Tiantian Li,¹ and Yunbo Zhang^{1,*}

¹*Institute of Theoretical Physics, Shanxi University, Taiyuan 030006, China*

²*Department of Physics, Taiyuan Normal University, Taiyuan 030001, China*

(Dated: March 4, 2022)

We present a variational study of pseudo-spin 1/2 Bose gases in a harmonic trap with weak 3D spin-orbit coupling of $\boldsymbol{\sigma} \cdot \mathbf{p}$ type. This spin-orbit coupling mixes states with different parities, which inspires us to approximate the single particle state with the eigenstates of the total angular momentum, i.e. superposition of harmonic s -wave and p -wave states. As the time reversal symmetry is protected by two-body interaction, we set the variational order parameter as the combination of two mutually time reversal symmetric eigenstates of the total angular momentum. The variational results essentially reproduce the 3D skyrmion-like ground state recently identified by Kawakami *et al.* We show that these skyrmion-like ground states emerging in this model are primarily caused by p wave spatial mode involving in the variational order parameter that drives two spin components spatially separated. We find the ground state of this system falls into two phases with different density distribution symmetries depending on the relative magnitude of intraspecies and interspecies interaction: Phase I has parity symmetric and axisymmetric density distributions, while Phase II is featured with special joint symmetries of discrete rotational and time reversal symmetry. With the increasing interaction strength the transition occurs between two phases with distinct density distributions, while the topological 3D skyrmion-like spin texture is symmetry protected.

PACS numbers: 67.85.Fg, 03.75.Mn, 67.85.Jk, 03.75.Lm

I. INTRODUCTION

The experimental realization [1, 2] of one-dimensional (1D) spin-orbit(SO) coupling in pseudo-spin 1/2 Bose gases has stimulated many theoretical works on SO coupling in cold atom physics. These works range from Raman induced 1D SO coupling [3–7] that has been realized in cold atoms to more symmetric two-dimensional (2D) Rashba configuration [7–15] that has been extensively studied in condensed matter. In the absence of harmonic trap, single particle ground states of both Raman induced and Rashba SO coupling are degenerate, and two-body interaction selects the generic ground state from the degenerate manifold determined by the interaction parameters. For example, Wang *et al.* [8] found two distinct ground state phases, namely the plane wave and standing wave(or stripe) phases, appeared when intraspecies two-body interaction is larger or smaller than interspecies interaction respectively in homogeneous 2D Rashba SO coupled pseudo-spin 1/2 Bose gases. In the presence of a 2D harmonic trap, a more complex phase diagram of Rashba SO coupled Bose gases with two classes of phases and several subphases in each was figured out by Hu *et al.* [9, 10].

Now experimental schemes for the realization of Rashba SO coupling have been proposed such as in Ref. [16]. On the other hand, the most symmetric three-dimensional (3D) SO coupling or Weyl coupling, which even doesn't exist in solid matter, is expected to be realizable in cold atoms gases and experimental schemes

for that have also been proposed theoretically [17, 18]. Recently, Kawakami *et al.* [19] identified a 3D skyrmion ground state in 3D SO coupled two-component bosons by numerically minimizing the Gross-Pitaevskii (GP) energy functional of the system. They explained the stability of 3D skyrmion ground state as a result of helical modulation of the order parameter in the presence of SO coupling. The interaction in their work is supposed to be SU(2) symmetric. Even though two skyrmion-like ground states are found to be stabilized in different interaction regimes, a ground state phase diagram is still absent now. In another work by Li *et al.* [20], the 3D skyrmion-like ground state is found to emerge in weak SO coupling regime, while skyrmion lattice arises in strong SO coupling regime.

In this work, we consider a pseudo-spin 1/2 boson system subject to 3D SO coupling of $\boldsymbol{\sigma} \cdot \mathbf{p}$ type in a harmonic trap, and aim to elucidate the role of interaction in determining the ground state density and spin texture therein. In Sec. II we introduce the energy functional for the model in rescaled units of length, energy, interaction and SO coupling strength. In weak SO coupling case, the single particle energy levels are essentially harmonic oscillator-like [21], and SO coupling will mix states with different parities while keeping the total angular momentum a conservative. In Sec III we first try to couple two lowest s and p wave states with the same total angular momentum 1/2 into two spinor wave functions with total angular momentum magnetic quantum number $\pm 1/2$ that are time reversal state of each other. Then we set the variational order parameter as superposition of these two states just as has been done in 1D and 2D cases [3, 8]. Finally, we calculate the energy functional using the proposed variational order parameter. In Sec IV

*Electronic address: ybzhang@sxu.edu.cn

the ground state phase diagram is determined by numerically minimizing the energy functional with respect to the variational parameters, we illustrate the density and spin texture for the two phases. Sec. V summarizes our main results.

II. MODEL

We consider a pseudo-spin 1/2 boson system confined in a harmonic trap with a weak Weyl type 3D spin-orbit (SO) coupling $\boldsymbol{\sigma} \cdot \mathbf{p}$. The system is described by its Gross-Pitaevskii (GP) energy functional under the mean-field approximation

$$\mathcal{E} = \mathcal{E}_0 + \mathcal{E}_{int}, \quad (1)$$

where the single particle part is

$$\mathcal{E}_0 = \int d^3\mathbf{r} \Psi^\dagger(\mathbf{r}) \left(\frac{\mathbf{p}^2}{2m} + \frac{1}{2}m\omega^2 r^2 + \lambda \boldsymbol{\sigma} \cdot \mathbf{p} \right) \Psi(\mathbf{r}) \quad (2)$$

with m the mass of atoms and ω the trap frequency. $\Psi = (\psi_\uparrow, \psi_\downarrow)^T$ denotes spinor order parameters for bosons with pseudo spin states \uparrow, \downarrow , $\boldsymbol{\sigma} = (\sigma_x, \sigma_y, \sigma_z)$ are the Pauli matrices and λ parameterizes the SO coupling strength. The interaction \mathcal{E}_{int} takes the usual contact form of s -wave scattering interaction [23]. We assume now [8–10, 20] the two intraspecies interaction parameters being the same $g_{\uparrow\uparrow} = g_{\downarrow\downarrow} = g$ and define the relative magnitude of the interspecies and intraspecies parameters as $c = g_{\uparrow\downarrow}/g_{\uparrow\uparrow}$. The interaction part is then

$$\mathcal{E}_{int} = \frac{1}{4} \int d^3\mathbf{r} ((g + cg)n^2 + 4(g - cg)S_z^2). \quad (3)$$

In Eq. (3), $n(\mathbf{r}) = n_\uparrow(\mathbf{r}) + n_\downarrow(\mathbf{r})$ is the particle density and S_z is the z component of the spin density $\mathbf{S} = \frac{1}{2}\Psi^\dagger \boldsymbol{\sigma} \Psi$ with $n_{\uparrow,\downarrow}(\mathbf{r}) = |\psi_{\uparrow,\downarrow}(\mathbf{r})|^2$ the particle densities of two components, respectively. The corresponding Hamiltonian is time-reversal (TR) symmetric with time reversal operator defined as $T = -i\sigma_y K$ and K denotes the complex conjugate. The system has length scale of the trapping potential $l_T = \sqrt{\hbar/m\omega}$, energy scale $\hbar\omega$, interaction strength scale $\hbar\omega l_T^3/N$, and SO coupling strength scale $\sqrt{\hbar\omega/m}$. If we further normalize the order parameter to unity, i.e., $\Psi \rightarrow \sqrt{N/l_T^3}\Psi$ with N the total particle number in the condensate, the energy functional per particle is obtained as

$$\epsilon = \int d^3\mathbf{r} \Psi^\dagger(\mathbf{r}) \left\{ -\frac{\nabla^2}{2} + \frac{r^2}{2} + \lambda \boldsymbol{\sigma} \cdot \mathbf{p} \right\} \Psi(\mathbf{r}) + \frac{1}{4} \int d^3\mathbf{r} ((g + cg)n^2 + 4(g - cg)S_z^2). \quad (4)$$

III. VARIATIONAL APPROACH

In the case of weak SO coupling the single particle energy spectrum in our system should be harmonic

oscillator-like as proposed in Ref. [20, 21]. The three dimensional harmonic oscillator thus proves to be a good choice of the trial wave function, upon which we may develop our variational method. As can be seen later the spin-orbit coupling induces transition between eigenstates with the same total angular momentum but different parity, which are mixed into the variational wave function. The interaction Hamiltonian further couples the two time-reversal states with different weight factor due to the anisotropic interaction parameter ratio c .

A. Variational order parameter

The eigenequation of three dimensional harmonic oscillator, $\left(-\frac{\nabla^2}{2} + \frac{r^2}{2}\right)\phi = \epsilon\phi$, has well-known solutions, with energy eigenvalues $\epsilon_{n_r, l} = 2n_r + l + \frac{3}{2}$ and eigenfunctions $\phi_{n_r, l, m_l}(r, \theta, \varphi) = R_{n_r, l}(r) Y_{l, m_l}(\theta, \varphi)$. Here n_r is the radial quantum number, l is the orbital angular momentum quantum number with m_l its magnetic quantum number, $R_{n_r, l}$ is the radial wave function, and Y_{l, m_l} is the spherical harmonics. The Casimir operator \mathbf{l}^2 and \mathbf{s}^2 for the orbital and spin angular momenta and their z -components are all conservatives in the harmonic oscillator problem. In order to take into account the spin-orbital coupling term $\boldsymbol{\sigma} \cdot \mathbf{p}$, it is convenient to choose the coupled representation of angular momentum, i.e. the complete set of commutative operators $\mathbf{l}^2, \mathbf{s}^2, \mathbf{j}^2, j_z$ where $\mathbf{j} = \mathbf{l} + \mathbf{s}$ and j_z denote the total angular momentum and its z -component, respectively. The eigenfunction $\phi_{n_r, l, m_l}(r, \theta, \varphi)$ should be combined with the spin wave function χ_{m_s} in the coupled representation as

$$\phi_{n_r, l, j, m_j}(r, \theta, \varphi) = R_{n_r, l}(r) Y_{l, m_l}^l(\Omega), \quad (5)$$

where $Y_{j, m_j}^l(\Omega) = \sum_{m_l, m_s} C_{l, m_l, \frac{1}{2} m_s}^{j, m_j} Y_{l, m_l} \chi_{m_s}$ is the spinor spherical harmonics [24] with $j = l \pm 1/2$ and $C_{l, m_l, \frac{1}{2} m_s}^{j, m_j}$ the Clebsch-Gordan coefficients. In the coupled representation, the ground state wave function has $n_r = l = 0$. This gives a total angular momentum $j = \frac{1}{2}$ with $m_j = \pm \frac{1}{2}$ and the two degenerate ground states are

$$\phi_{00, \frac{1}{2} \pm \frac{1}{2}}(\mathbf{r}) = R_{00}(r) Y_{\frac{1}{2} \pm \frac{1}{2}}^0(\Omega), \quad (6)$$

respectively. Because the SO coupling term breaks the parity symmetry, it can couple s and p wave states with the same total angular momentum \mathbf{j} and j_z [20]. Keeping these consideration in mind, in the simplest approximation, we suppose the ground state contains only the lowest s and p wave states with total angular momentum quantum number $j = \frac{1}{2}$ in presence of the SO coupling term. The state with $m_j = \frac{1}{2}$ takes the form

$$\Phi_{j=\frac{1}{2}, m_j=\frac{1}{2}} = N_\alpha \left(\phi_{00, \frac{1}{2} \pm \frac{1}{2}} + i\alpha \phi_{01, \frac{1}{2} \pm \frac{1}{2}} \right) \quad (7)$$

where $N_\alpha = (1 + \alpha^2)^{-1/2}$, α stands for the relative weight of the s and p orbital modes, and i in front of α originates

from the pure imaginary matrix element of the SO coupling between the two states in Eq. (7). This hypothesis is similar to that appears in Refs. [20] and [21], and has been verified numerically [20]. Explicitly this state is a spinor

$$\Phi_{j=\frac{1}{2}, m_j=\frac{1}{2}} = N_\alpha \begin{pmatrix} R_{00}Y_{00} - i\alpha\sqrt{\frac{1}{3}}R_{01}Y_{10} \\ i\alpha\sqrt{\frac{2}{3}}R_{01}Y_{11} \end{pmatrix}. \quad (8)$$

The state with $m_j = -\frac{1}{2}$ takes the form

$$\Phi_{j=\frac{1}{2}, m_j=-\frac{1}{2}} = N_\alpha \left(\phi_{00\frac{1}{2}-\frac{1}{2}} + i\alpha\phi_{01\frac{1}{2}-\frac{1}{2}} \right) \quad (9)$$

and similarly we have

$$\Phi_{j=\frac{1}{2}, m_j=-\frac{1}{2}} = N_\alpha \begin{pmatrix} -i\alpha\sqrt{\frac{2}{3}}R_{01}Y_{1-1} \\ R_{00}Y_{00} + i\alpha\sqrt{\frac{1}{3}}R_{01}Y_{10} \end{pmatrix} \quad (10)$$

which is nothing but the time reversal of $\Phi_{j=\frac{1}{2}, m_j=\frac{1}{2}}$. In the single particle level, $\Phi_{j=\frac{1}{2}, m_j=\pm\frac{1}{2}}$ and any normalized superposition of them has the same energy thus are “degenerate” single particle states, which is similar to degeneracy indicated by Kramers’ theorem in spin-1/2 system.

The single particle states exhibit infinite-fold degeneracy and we expect this degeneracy can be partially resolved by the interaction which would pick up the ground state from these degenerate states as in the case of Rashba spin-orbital coupling considered by Wang and Zhai [8]. Since the interaction doesn’t break the time reversal symmetry, the residual two-fold Kramers degeneracy need to be considered in the wave function [2]. We therefore set the variational order parameter as

$$\begin{aligned} \Psi &= c_+ \Phi + c_- T\Phi \\ &= \begin{pmatrix} c_+ \Phi_\uparrow - c_- \Phi_\downarrow^* \\ c_+ \Phi_\downarrow + c_- \Phi_\uparrow^* \end{pmatrix}, \end{aligned} \quad (11)$$

with the constraint $c_+^2 + c_-^2 = 1$. Here $\Phi \equiv \Phi_{j=\frac{1}{2}, m_j=\frac{1}{2}}$ and $\Phi_{\uparrow, \downarrow}$ are its up and down components. So far, we have introduced three variational parameters α, c_+, c_- and the energy functional of Eq. (4) can be calculated analytically using the proposed order parameter (11).

B. Energy functional

We calculate the energy functional on the variational wave function (11). The contribution comes from two parts, the single particle and the interaction Hamiltonian. We notice that for the kinetic and trapping potential terms the nonzero integral contribution comes from those states with the same parities, while spin orbital

coupling $\boldsymbol{\sigma} \cdot \mathbf{p}$ term will mix states with opposite parities, i.e.

$$\begin{aligned} &\int d^3\mathbf{r} \Psi^\dagger(\mathbf{r}) \left\{ -\frac{\nabla^2}{2} + \frac{r^2}{2} + \lambda \boldsymbol{\sigma} \cdot \mathbf{p} \right\} \Psi(\mathbf{r}) \\ &= N_\alpha^2 \left[\left\langle \phi_{00\frac{1}{2}\frac{1}{2}} \left| \left(-\frac{\nabla^2}{2} + \frac{r^2}{2} \right) \right| \phi_{00\frac{1}{2}\frac{1}{2}} \right\rangle \right. \\ &\quad + \alpha^2 \left\langle \phi_{01\frac{1}{2}\frac{1}{2}} \left| \left(-\frac{\nabla^2}{2} + \frac{r^2}{2} \right) \right| \phi_{01\frac{1}{2}\frac{1}{2}} \right\rangle \\ &\quad \left. + i2\alpha \left\langle \phi_{00\frac{1}{2}\frac{1}{2}} \left| \lambda \boldsymbol{\sigma} \cdot \mathbf{p} \right| \phi_{01\frac{1}{2}\frac{1}{2}} \right\rangle \right]. \end{aligned} \quad (12)$$

Here we have used

$$\begin{aligned} &\left\langle \phi_{00\frac{1}{2}\frac{1}{2}} \left| \lambda \boldsymbol{\sigma} \cdot \mathbf{p} \right| \phi_{01\frac{1}{2}\frac{1}{2}} \right\rangle \\ &= \left\langle \phi_{00\frac{1}{2}-\frac{1}{2}} \left| \lambda \boldsymbol{\sigma} \cdot \mathbf{p} \right| \phi_{01\frac{1}{2}-\frac{1}{2}} \right\rangle, \end{aligned} \quad (13)$$

which is on account of $[j_z, \boldsymbol{\sigma} \cdot \mathbf{p}] = 0$.

It is crucial to calculate the contribution of the spin-orbital coupling term by means of the irreducible tensor method [24]. To this end we first introduce the irreducible form of spin-orbital coupling term. The irreducible tensor form of momentum operator is [24]

$$p^{(1)} = i\sqrt{2}\frac{1}{r} \left\{ C^{(1)} l^{(1)} \right\}^{(1)} - i\frac{\partial}{\partial r} C^{(1)}, \quad (14)$$

where $C^{(1)}$ and $l^{(1)}$ are rank-1 irreducible tensors of the unit vector $\hat{\mathbf{r}}$ and the orbital angular momentum \mathbf{l} , and $\{A^{(m)} B^{(n)}\}^{(k)}$ defines the rank- k tensor product of rank- m irreducible tensor $A^{(m)}$ and rank- n irreducible tensor $B^{(n)}$. According to [24], the dot product of two arbitrary vectors \mathbf{A} and \mathbf{B} is related to the tensor product through $\mathbf{A} \cdot \mathbf{B} = -\sqrt{3} \{A^{(1)} B^{(1)}\}^{(0)}$. In our case, the radial coordinate r can be separated from the spin and spherical parts accordingly

$$\begin{aligned} \boldsymbol{\sigma} \cdot \mathbf{p} &= -i\frac{\sqrt{6}}{r} \left\{ \sigma^{(1)} \left\{ C^{(1)} l^{(1)} \right\}^{(1)} \right\}^{(0)} \\ &\quad + i\sqrt{3} \frac{\partial}{\partial r} \left\{ \sigma^{(1)} C^{(1)} \right\}^{(0)}, \end{aligned} \quad (15)$$

such that

$$\begin{aligned} &\left\langle \phi_{00\frac{1}{2}\frac{1}{2}} \left| \boldsymbol{\sigma} \cdot \mathbf{p} \right| \phi_{01\frac{1}{2}\frac{1}{2}} \right\rangle \\ &= -i\sqrt{6} \left\langle R_{00}(r) \left| \frac{1}{r} \right| R_{01}(r) \right\rangle \\ &\quad \times \left\langle Y_{\frac{1}{2}\frac{1}{2}}^0(\Omega) \left| \left\{ \sigma^{(1)} \left\{ C^{(1)} l^{(1)} \right\}^{(1)} \right\}^{(0)} \right| Y_{\frac{1}{2}\frac{1}{2}}^1(\Omega) \right\rangle \\ &\quad + i\sqrt{3} \left\langle R_{00}(r) \left| \frac{d}{dr} \right| R_{01}(r) \right\rangle \\ &\quad \times \left\langle Y_{\frac{1}{2}\frac{1}{2}}^0(\Omega) \left| \left\{ \sigma^{(1)} C^{(1)} \right\}^{(0)} \right| Y_{\frac{1}{2}\frac{1}{2}}^1(\Omega) \right\rangle. \end{aligned} \quad (16)$$

The integrals for the radial coordinates are easy to calculate,

$$\left\langle R_{00}(r) \left| \frac{1}{r} \right| R_{01}(r) \right\rangle = \sqrt{\frac{2}{3}}, \quad (17)$$

$$\left\langle R_{00}(r) \left| \frac{d}{dr} \right| R_{01}(r) \right\rangle = -\frac{1}{\sqrt{6}}, \quad (18)$$

where $R_{00}(r) = \sqrt{2^2/\sqrt{\pi}}e^{-r^2/2}$ and $R_{01}(r) = \sqrt{2^3/(3\sqrt{\pi})}re^{-r^2/2}$ are used. Wigner-Eckart theorem can be used to calculate the angular and spin integral

$$\left\langle Y_{\frac{1}{2}\frac{1}{2}}^0(\Omega) \left| \left\{ \sigma^{(1)} \left\{ C^{(1)} l^{(1)} \right\}^{(1)} \right\}^{(0)} \right| Y_{\frac{1}{2}\frac{1}{2}}^1(\Omega) \right\rangle = \frac{1}{\sqrt{6}}, \quad (19)$$

$$\left\langle Y_{\frac{1}{2}\frac{1}{2}}^0(\Omega) \left| \left\{ \sigma^{(1)} C^{(1)} \right\}^{(0)} \right| Y_{\frac{1}{2}\frac{1}{2}}^1(\Omega) \right\rangle = \frac{1}{\sqrt{3}}. \quad (20)$$

Substitute Eq. (17-20) into Eq. (16), one has

$$\left\langle \phi_{00\frac{1}{2}\frac{1}{2}} | \boldsymbol{\sigma} \cdot \mathbf{p} | \phi_{01\frac{1}{2}\frac{1}{2}} \right\rangle = -i\sqrt{\frac{3}{2}}. \quad (21)$$

Hence the single particle part of the energy functional is

$$\begin{aligned} & \int d^3\mathbf{r} \Psi^\dagger(\mathbf{r}) \left\{ -\frac{\nabla^2}{2} + \frac{r^2}{2} + \lambda \boldsymbol{\sigma} \cdot \mathbf{p} \right\} \Psi(\mathbf{r}) \\ &= N_\alpha^2 \left(\frac{3}{2} + \frac{5}{2}\alpha^2 + \sqrt{6}\alpha\lambda \right) \end{aligned} \quad (22)$$

where we have used the eigen energies of the s and p states of the three dimensional oscillator are respectively $\varepsilon_{00} = 3/2$ and $\varepsilon_{01} = 5/2$.

For the calculation of the interaction part of energy functional, it is easy to show that the total density n is always spherical symmetric

$$n = |\Phi|^2 = (4\pi)^{-1} N_\alpha^2 (R_{00}^2 + \alpha^2 R_{01}^2), \quad (23)$$

and the density-density interaction energy is

$$\int d^3\mathbf{r} n^2 = \frac{1}{12} N_\alpha^4 (2\pi)^{-\frac{3}{2}} (5\alpha^4 + 12\alpha^2 + 12). \quad (24)$$

On the other hand, the spin density is anisotropic, e.g. the z component takes the form of

$$\begin{aligned} S_z &= (8\pi)^{-1} N_\alpha^2 \{ (c_+^2 - c_-^2) (R_{00}^2 + \alpha^2 R_{01}^2 \cos 2\theta) \\ &\quad - (2c_+ c_-) (2\alpha R_{00} R_{01} \sin \theta \sin \varphi - \alpha^2 R_{01}^2 \sin 2\theta \cos \varphi) \}, \end{aligned} \quad (25)$$

and the spin-spin interaction energy is integrated as

$$\begin{aligned} & \int d^3\mathbf{r} S_z^2 = \frac{1}{4} N_\alpha^4 (2\pi)^{-\frac{3}{2}} \left[\frac{1}{36} (7\alpha^4 - 12\alpha^2 + 36) \right. \\ & \quad \left. - \frac{1}{3} c_+^2 c_-^2 (\alpha^4 - 12\alpha^2 + 12) \right]. \end{aligned} \quad (26)$$

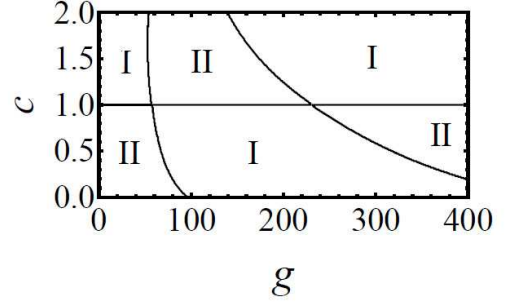


FIG. 1: Phase diagram of weakly SO coupled two-component Bosons with coupling strength $\lambda = 0.2$, which shows two skyrmion-like phases I and II. Phase I is a skyrmion ground state of order parameter $\exp[-i\boldsymbol{\Omega}(\mathbf{r}) \cdot \mathbf{S}] \boldsymbol{\zeta}$ with $\boldsymbol{\zeta}_z = (1, 0)^T$ and Phase II is a skyrmion state with $\boldsymbol{\zeta}_x = \frac{1}{\sqrt{2}}(1, 1)^T$. Density distribution and spin texture of these two phases are shown in Fig. 2 and Fig. 3 respectively.

Collecting Eqs. (22), (24) and (26) into Eq. (4), we finally arrive at the variational result for the ground state energy per particle

$$\begin{aligned} \epsilon &= N_\alpha^2 \left(\frac{3}{2} + \frac{5}{2}\alpha^2 + \sqrt{6}\alpha\lambda \right) \\ &\quad + N_\alpha^4 (2\pi)^{-\frac{3}{2}} \frac{1}{72} \left[(11\alpha^4 + 12\alpha^2 + 36)g + (4\alpha^4 + 24\alpha^2)cg \right. \\ &\quad \left. - 6c_+^2 c_-^2 (g - cg) (\alpha^4 - 12\alpha^2 + 12) \right]. \end{aligned} \quad (27)$$

IV. GROUND STATE PHASE DIAGRAM

The ground state phase diagram can be determined numerically via the minimization of the variational energy with respect to the parameters α , c_+ and c_- for given c and g . We notice that the parameters c_+ and c_- appear only in the last term of Eq. (27) in the form of $c_+^2 c_-^2$, the value of which ranges from 0 to 1/4. The parameter $c_+^2 c_-^2$ as a whole takes the value of either 0 or 1/4 in the minimization, depending on the signs of $(g - cg)$ and $f(\alpha) = \alpha^4 - 12\alpha^2 + 12$. The ground state thus falls into two classes of phases as depicted in FIG. 1: Phase I, the variation yields $|c_+|^2 = 1$, $|c_-|^2 = 0$ or $|c_+|^2 = 0$, $|c_-|^2 = 1$; Phase II, the variation yields $|c_+|^2 = |c_-|^2 = 1/2$. It is clear that α must be negative for a positive λ due to the fact that α 's in Eq. (27) are all even-ordered except the spin-orbital coupling term. We see that $c = 1$ divides the phase plane into upper and lower regions. With increasing g the system enters alternately into Phases I and II and the boundaries are determined by $f(\alpha) = 0$, i.e. $\alpha_{\pm} = -\sqrt{6} \pm 2\sqrt{6}$. For typical experiments with ^{87}Rb condensate, the interaction strength scale is 10^{-13}Hzcm^3 , which gives rise to $g \sim 40 - 80$. For smaller g , $\alpha \geq \alpha_-$ results in a positive value of $f(\alpha)$ such that $c > 1$ region belongs to

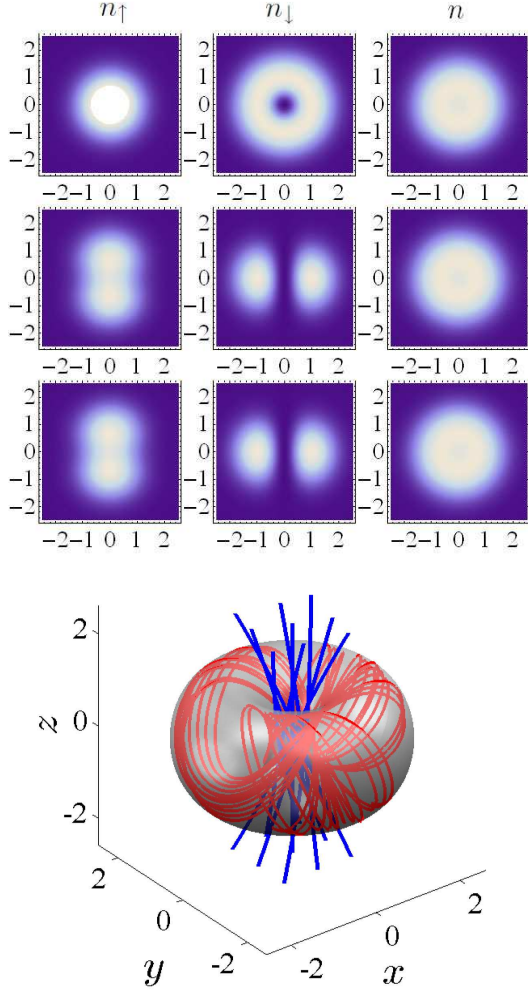


FIG. 2: (Color online). Density distribution and spin texture of Phase I for $\alpha = -1.6$. Top: Three rows are densities in xy , yz and xz planes respectively, three columns are for up, down components and the total density as explicitly labeled above each column. Density distributions in xz and yz plane are the same due to the z -axis rotational symmetry. Bottom: 3D skyrmion spin texture $\mathbf{s}(\mathbf{r}) = \mathbf{S}(\mathbf{r})/n(\mathbf{r})$ of Phase I. The streamline plot of \mathbf{s} in a selected region are shown.

Phase I and $c < 1$ belongs to Phase II. By adjusting the trapping frequency and the density of the condensate one can easily increase g to cross the critical line such that $\alpha \in [\alpha_+, \alpha_-]$, which makes $f(\alpha)$ negative. We observe an interesting swap of the phases: $c < 1$ corresponds to Phase I and $c > 1$ corresponds to Phase II. Similar phase transition appears in the Rashba spin-orbital coupled Bosons [9, 10]. Further increasing the interaction strength makes the optimized parameter $\alpha \leq \alpha_+$ and the phases swap occurs again.

The density distributions and the spin texture of Phases I and II are shown in Figs. 2 and 3, respectively. Typical features include:

Phase I: this phase contains two degenerate states $|c_+|^2 = 1$, $|c_-|^2 = 0$ and $|c_+|^2 = 0$, $|c_-|^2 = 1$. They are

time reversal states of each other and have similar density and spin texture except that the spin-up and spin-down components are exchanged. The order parameter for the former has the form

$$\Psi = (4\pi)^{-\frac{1}{2}} N_\alpha \begin{pmatrix} R_{00}(r) - i\alpha R_{01}(r) \cos \theta \\ -i\alpha R_{01}(r) \sin \theta e^{i\varphi} \end{pmatrix}.$$

The particle densities for the spin-up and spin-down components are

$$\begin{aligned} n_\uparrow &= (4\pi)^{-1} N_\alpha^2 (R_{00}^2(r) + \alpha^2 R_{01}^2(r) \cos^2 \theta), \\ n_\downarrow &= (4\pi)^{-1} N_\alpha^2 \alpha^2 R_{01}^2(r) \sin^2 \theta, \end{aligned} \quad (28)$$

which respect the rotational symmetry about z -axis and the parity symmetry, i.e. $n_{\uparrow,\downarrow}(\mathbf{r}) = n_{\uparrow,\downarrow}(r, \theta)$ and $n_{\uparrow,\downarrow}(r, \theta) = n_{\uparrow,\downarrow}(r, \pi - \theta)$. The densities of the two components in xz and yz planes are the same as shown in Fig. 2, which exhibit clearly characters of the p wave state, i.e. the spin-up component is dumbbell-like while the spin-down component forms a torus. The total density on the other hand is isotropic - the sum of n_\uparrow and n_\downarrow in Eq. (28) relies only on the radius r .

This spin density calculated on the variational order parameter shows interesting spin texture described by

$$\begin{aligned} S_x &= (4\pi)^{-1} N_\alpha^2 (\alpha R_{00}(r) R_{01}(r) \sin \theta \sin \varphi \\ &\quad + \alpha^2 R_{01}^2(r) \sin \theta \cos \theta \cos \varphi), \\ S_y &= (4\pi)^{-1} N_\alpha^2 (-\alpha R_{00}(r) R_{01}(r) \sin \theta \cos \varphi \\ &\quad + \alpha^2 R_{01}^2(r) \sin \theta \cos \theta \sin \varphi), \\ S_z &= (8\pi)^{-1} N_\alpha^2 (R_{00}^2(r) + \alpha^2 R_{01}^2(r) \cos 2\theta). \end{aligned} \quad (29)$$

The average value of the spin in the xy plane is zero, i.e. $\langle S_x \rangle = \langle S_y \rangle = 0$. The spin texture $\mathbf{s}(\mathbf{r}) = \mathbf{S}(\mathbf{r})/n(\mathbf{r})$ is depicted in Fig. 2 and we find that spin density forms a torus near the xy plane and a bundle of nearly vertical streamlines of spin penetrate the central region of the torus. This skyrmion-like texture has been discussed in Ref. [19] and identified as the ground state in $c < 1$ regime for an interaction parameter $c_0 = 100$. Li *et al.* [20] also found this ground state skyrmion spin texture in weak SO coupling case for isotropic interaction $c = 1$. The term “skyrmion-like” means the absence of boundary condition at $r \rightarrow \infty$ [19] thus the winding number for the texture is not an integer.

In order to get a deep understanding of the skyrmion nature of this ground state, we notice that the order parameter can be obtained from a local spin rotation from the polarized spinor wavefunction $\zeta_z = (c_+, c_-)^T = (1, 0)^T$

$$\Psi_z = \exp(-i\mathbf{\Omega}(\mathbf{r}) \cdot \mathbf{s}) \sqrt{n(\mathbf{r})} \zeta_z \quad (30)$$

supposing that $n(\mathbf{r}) = (4\pi)^{-1} N_\alpha^2 (R_{00}^2(r) + \alpha^2 R_{01}^2(r))$ and $\mathbf{\Omega}(\mathbf{r}) = \omega(r) \mathbf{r}/r$. This operation rotates the spin at position \mathbf{r} by an angle $\omega(r)$ about the axis \mathbf{r}/r . The rotation angle is position dependent, i.e. $\omega(r) =$

$2 \arctan(\alpha R_{01}(r)/R_{00}(r))$ and \mathbf{s} is the usual spin angular momentum operators for spin-1/2. It is the explicit form of $\mathbf{\Omega}(\mathbf{r})$ that determines the specific texture of the skyrmion [22]. The polarized spinor order parameter ζ_z has all spins being oriented in the positive z -direction. After the rotation the order parameter Ψ_z for this skyrmion state is position-dependent. The order parameter is the most symmetrically shaped skyrmion with the symmetric axis unrotated, which is identical with that already discussed in Refs. [22, 25–29]. In those papers the 3D skyrmion states are proposed as excited states in pseudo-spin 1/2 or ferromagnetic spin-1 [22] Bose gases although they may be metastable.

Phase II: this phase again contains two degenerate states with $c_+ = c_- = \pm \frac{1}{\sqrt{2}}$ and $c_+ = -c_- = \pm \frac{1}{\sqrt{2}}$, which are time reversal states of each other. They share similar density distribution and spin texture just like the case of Phase I. The order parameter for $c_+ = c_-$ has the form

$$\Psi = (8\pi)^{-\frac{1}{2}} N_\alpha \begin{pmatrix} R_{00}(r) - i\alpha R_{01}(r) (\cos\theta + \sin\theta e^{-i\varphi}) \\ R_{00}(r) - i\alpha R_{01}(r) (-\cos\theta + \sin\theta e^{i\varphi}) \end{pmatrix}, \quad (31)$$

and the particle densities for the two components are

$$\begin{aligned} n_\uparrow &= (8\pi)^{-1} N_\alpha^2 (R_{00}^2(r) + \alpha^2 R_{01}^2(r) \\ &\quad - 2\alpha R_{00} R_{01} \sin\theta \sin\varphi + \alpha^2 R_{01}^2 \sin 2\theta \cos\varphi), \\ n_\downarrow &= (8\pi)^{-1} N_\alpha^2 (R_{00}^2(r) + \alpha^2 R_{01}^2(r) \\ &\quad + 2\alpha R_{00} R_{01} \sin\theta \sin\varphi - \alpha^2 R_{01}^2 \sin 2\theta \cos\varphi). \end{aligned} \quad (32)$$

The density for each component consists of two parts, one is isotropic that is common for both components, the other is complementary to each other as shown in the second and fourth lines in Eq. (32). This leads again to an isotropic total density. The overall density distribution of the two components can be visualized as two cashew nuts perpendicularly crossing and partially overlapping with each other. The distributions in xy , yz and xz planes are shown in Fig. 3. The density distributions have the following symmetries, e.g., the densities of two components are invariant under the combined operation of time reversal and π rotation about x (or z) axis, i.e. $n_\uparrow(r, \pi - \theta, 2\pi - \phi) = n_\downarrow(r, \theta, \phi)$, $n_\uparrow(r, \theta, \pi + \phi) = n_\downarrow(r, \theta, \phi)$, while the π rotation about y axis itself leaves the density distributions unchanged, i.e. $n_{\uparrow,\downarrow}(r, \pi - \theta, \pi - \phi) = n_{\uparrow,\downarrow}(r, \theta, \phi)$.

The spin texture associated with the order parameter is expressed as

$$\begin{aligned} S_x &= (8\pi)^{-1} N_\alpha^2 \times \\ &\quad (R_{00}^2 + \alpha^2 R_{01}^2 (\sin^2\theta \cos 2\varphi - \cos^2\theta)), \\ S_y &= (8\pi)^{-1} N_\alpha^2 \times \\ &\quad (2\alpha R_{00} R_{01} \cos\theta + \alpha^2 R_{01}^2 \sin^2\theta \sin 2\varphi), \\ S_z &= (8\pi)^{-1} N_\alpha^2 \times \\ &\quad (-2\alpha R_{00} R_{01} \sin\theta \sin\varphi + \alpha^2 R_{01}^2 \sin 2\theta \cos\varphi). \end{aligned} \quad (33)$$

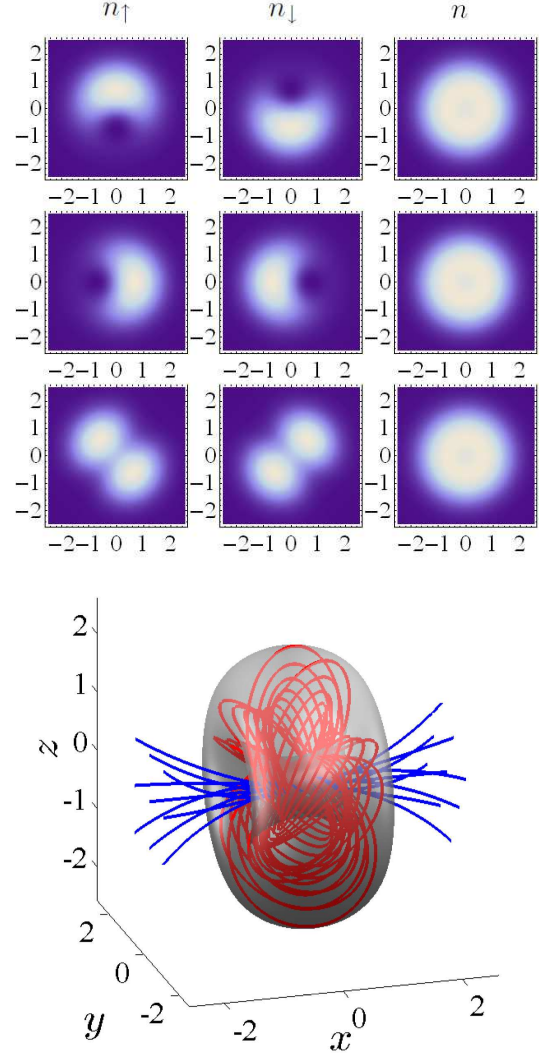


FIG. 3: (Color online). Density distribution and spin texture of Phase II for $\alpha = -1.6$. Top: Three rows are densities in xy , yz and xz planes respectively, three columns are for up, down components and the total density as explicitly labeled above each column. Though the total density is isotropic again, the density distribution for the two components exhibits more complex symmetry as described in the text. Bottom: 3D skyrmion spin texture $\mathbf{s}(\mathbf{r}) = \mathbf{S}(\mathbf{r})/n(\mathbf{r})$ of Phase II, which is roughly a $\pi/2$ rotation about y -axis of that in Phase I. The topological structure of the spin texture is protected by the time reversal symmetry.

The average spin polarization along z axis is zero, i.e. $\langle S_z \rangle = 0$. The spin texture $\mathbf{S}(\mathbf{r})/n(\mathbf{r})$ is presented in Fig. 3. The spin density in this case forms a torus near the yz plane and the fountain-like streamlines of spin pass through the hole of the torus, which is more or less like a $\pi/2$ rotation of the torus in Phase I about y axis. Similarly, this ground state can be obtained from a local spin rotation from the spinor order parameter $\zeta_x = (c_+, c_-)^T = \frac{1}{\sqrt{2}}(1, 1)^T$ that describes a system with

all spins pointing to the positive x direction, i.e.

$$\Psi_x = \exp(-i\mathbf{\Omega}(\mathbf{r}) \cdot \mathbf{s}) \sqrt{n(\mathbf{r})} \zeta_x. \quad (34)$$

The spinor wavefunction ζ_x is related to ζ_z by a $\pi/2$ rotation around y . Owing to the non-Abelian nature of SO(3) rotation, the spin texture of Phase II is different from the $\pi/2$ rotation around y of Phase I. The difference between these two textures lies in the fact that the spin in the torus of Phase I revolves the z axis following an elliptical (oval) orbits that rotate gradually like the perihelion precession in celestial mechanics, while in Phase II the orbits are closed loops. Apart from this, they indeed share the same topology determined by the same $\mathbf{\Omega}$ as can be seen from the spin streamline plot in Fig. 3, because the topological spin texture is protected by time reversal symmetry of the system. This skyrmion spin texture is proposed as the ground state in the regime of $c > 1$ in Ref. [19].

We find in this study that in both phase I and phase II, the densities of the two components are spatially separated in three dimensions. We thus come up with a conclusion that phase separation of the spin components generally exists in 1D[30], 2D[9, 10] and 3D SO coupled Boson gases. In our case it is the SOC-induced p wave spatial mode involving in the variational order parameter that drives the two spin components spatially separated. As pointed out by Battye *et al.* [31] phase separation is a prerequisite for existence of stable skyrmion, which explains why skyrmion spin texture appears in the variational ground state of our model. Furthermore the topology of the skyrmion texture is protected by the time reversal symmetry of the system even the phase transition drastically changes the density structure.

V. SUMMARY

We have investigated variationally the ground state phase diagram of weakly 3D spin-orbital coupled two-component Bose gases in a harmonic trap. Two phases for the ground state are identified depending on intraspecies and interspecies interaction strength and the corresponding density distribution and the spin texture are illustrated for optimized variational parameters. Phase I is featured with the parity symmetric and rotational symmetric density distribution of both spin-up and spin-down components and skyrmion spin texture with torus in the xy plane and spin streamline passing through the central region, while Phase II is characterized with density distribution possessing discrete π rotational symmetry about y axis and π rotational-time-reversal symmetry about x and z axis and the similar spin torus is in the yz plane, roughly a $\pi/2$ rotation of that in Phase I about y axis. In both phases, the density of two components is essentially phase separated. With increasing interaction strength, interesting phase transition occurs between the two phases, while the topology of ground state spin textures is protected.

Acknowledgments

This work is supported by NSF of China under Grant Nos. 11234008 and 11474189, the National Basic Research Program of China (973 Program) under Grant No. 2011CB921601, Program for Changjiang Scholars and Innovative Research Team in University (PCSIRT)(No. IRT13076).

-
- [1] Y.-J. Lin, K. Jimenez-Garcia, and I. Spielman, *Nature*(London) **471**, 83 (2011).
 - [2] V. Galitski and I. B. Spielman, *Nature* **494**, 49 (2013).
 - [3] T.-L. Ho and S. Zhang, *Phys. Rev. Lett.* **107**, 150403 (2011).
 - [4] Y. Li, L. P. Pitaevskii, and S. Stringari, *Phys. Rev. Lett.* **108**, 225301 (2012).
 - [5] W. Zheng, Z.-Q. Yu, X. Cui, and H. Zhai, *Journal of Physics B: Atomic, Molecular and Optical Physics* **46**, 134007 (2013).
 - [6] Z. Chen and H. Zhai, *Phys. Rev. A* **86**, 041604 (2012).
 - [7] H. Zhai, *arXiv preprint arXiv:1403.8021* (2014).
 - [8] C. Wang, C. Gao, C.-M. Jian, and H. Zhai, *Phys. Rev. Lett.* **105**, 160403 (2010).
 - [9] H. Hu, B. Ramachandhran, H. Pu, and X.-J. Liu, *Phys. Rev. Lett.* **108**, 010402 (2012).
 - [10] B. Ramachandhran, B. Opanchuk, X.-J. Liu, H. Pu, P. D. Drummond, and H. Hu, *Phys. Rev. A* **85**, 023606 (2012).
 - [11] Y. Zhang, L. Mao, and C. Zhang, *Phys. Rev. Lett.* **108**, 035302 (2012).
 - [12] Z.-Q. Yu, *Phys. Rev. A* **87**, 051606 (2013).
 - [13] H. Zhai, *International Journal of Modern Physics B* **26**, 1230001 (2012).
 - [14] X. Cui and Q. Zhou, *Phys. Rev. A* **87**, 031604 (2013).
 - [15] Q. Zhou and X. Cui, *Phys. Rev. Lett.* **110**, 140407 (2013).
 - [16] D. L. Campbell, G. Juzeliūnas, and I. B. Spielman, *Phys. Rev. A* **84**, 025602 (2011).
 - [17] B. Anderson, G. Juzeliūnas, V. Galitski, and I. Spielman, *Phys. Rev. Lett.* **108**, 235301 (2012).
 - [18] B. Anderson, I. Spielman, and G. Juzeliūnas, *Phys. Rev. Lett.* **111**, 125301 (2013).
 - [19] T. Kawakami, T. Mizushima, M. Nitta, and K. Machida, *Phys. Rev. Lett.* **109**, 015301 (2012).
 - [20] Y. Li, X. Zhou, and C. Wu, *arXiv preprint arXiv:1205.2162* (2012).
 - [21] B. M. Anderson and C. W. Clark, *Journal of Physics B: Atomic, Molecular and Optical Physics* **46**, 134003 (2013).
 - [22] U. Khawaja and H. Stoof, *Phys. Rev. A* **64**, 043612 (2001).
 - [23] T.-L. Ho and V. Shenoy, *Phys. Rev. Lett.* **77**, 3276 (1996).
 - [24] D. Varshalovich, A. Moskalev, and V. Khersonskii, *Quantum Theory of Angular Momentum* (World Scientific, Singapore, 1988).
 - [25] U. Al Khawaja and H. Stoof, *Nature* **411**, 918 (2001).

- [26] J. Ruostekoski and J. Anglin, Phys. Rev. Lett. **86**, 3934 (2001).
- [27] C. Savage and J. Ruostekoski, Phys. Rev. Lett. **91**, 010403 (2003).
- [28] I. Herbut and M. Oshikawa, Phys. Rev. Lett. **97**, 080403 (2006).
- [29] A. Tokuno, Y. Mitamura, M. Oshikawa, and I. Herbut, Phys. Rev. A **79**, 053626 (2009).
- [30] S. Gautam and S. K. Adhikari, Phys. Rev. A **90**, 043619 (2014).
- [31] R. Battye, N. Cooper, and P. Sutcliffe, Phys. Rev. Lett. **88**, 080401 (2002).